The Cryosphere Discuss., 7, 35–53, 2013
www.the-cryosphere-discuss.net/7/35/2013/
doi:10.5194/tcd-7-35-2013

The Cryosphere Discussions

New estimates of Arctic and Antarctic sea ice extent during September 1964 from recovered Nimbus I satellite imagery

W. N. Meier, D. Gallaher, and G. G. Campbell

National Snow and Ice Data Center, UCB 449, University of Colorado, Boulder, Colorado, 80309 USA

Received: 27 November 2012 – Accepted: 10 December 2012 – Published: 2 January 2013

Correspondence to: W. N. Meier (walt@nsidc.org)

Published by Copernicus Publications on behalf of the European Geosciences Union.

Abstract

Satellite imagery from the 1964 Nimbus I satellite has been recovered, digitized, and processed to estimate Arctic and Antarctic sea ice extent for September 1964. September is the month when the Arctic reaches its minimum annual extent and the Antarctic reaches its maximum. Images were manually analyzed over a three-week period to estimate the location of the ice edge and then composited to obtain a hemispheric average. Uncertainties were based on limitations in the image analysis and the variation of the ice cover over the three week period. The 1964 Antarctic extent is higher than estimates from the 1979–present passive microwave record, but is in accord with previous indications of higher extents during the 1960s. The Arctic 1964 extent was near the 1979–2000 average from the passive microwave record, suggesting relatively stable summer extents until the recent large decrease. This early satellite record puts the recently observed into a longer-term context.

1 Introduction

The decline of Arctic sea ice extent over the past 3+ decades is one of the iconic indicators of climate change, culminating with a record low minimum extent in September 2012. The primary source these sea ice extent estimates are a series of multi-channel passive microwave radiometers, the Scanning Multichannel Microwave Radiometer SMMR) aboard the NASA Nimbus-7 platform and a succession of Special Sensor Microwave/Imager (SSM/I) sensors on US Department of Defense Meteorological Satellite Program (DMSP) satellites. Several algorithms, such as the NASA Team (Cavalieri et al., 1984) and Bootstrap (Comiso, 1986) have been developed to derive sea ice concentration and extent from estimated passive microwave brightness temperatures. For sensor transitions, algorithm coefficients are adjusted to provide intercalibration across sensor transitions (e.g. Cavalieri et al., 2012) to provide a consistent timeseries through the multi-channel passive microwave sensor record.

TCD
7, 35–53, 2013

This record, starting in late 1978, has provided invaluable information on long-term trends and variability in sea ice extent in both the Arctic (Parkinson and Cavalieri, 2008; Comiso and Nishio, 2008) and Antarctic (Cavalieri and Parkinson, 2008; Comiso and Nishio, 2008). The data indicate strong downward trends in all seasons and most regions of the Arctic. The Antarctic is a more complicated situation with overall increasing trends in hemispheric sea ice extent, but with large interannual and regional variability.

A limitation of these data is that they extend back only to 1978. Longer timeseries are desired to investigate longer-term climate trends and to provide longer records for comparison and inputs into climate models. For example, there are anecdotal indications that Antarctic sea ice extent was larger during the 1960s and the 30 yr increasing trend is a return toward those conditions. In the Arctic, a downward trend is evident, particularly during summer, almost from the beginning of the passive microwave record. Earlier data would put these trends into longer-term context.

There are a few earlier sources of sea ice extent information. A single-channel microwave radiometer flown on Nimbus-5, the Electronically Scanning Microwave Radiometer (ESMR), provides data from 1972–1977. However, the single channel algorithm is not consistent with the multi-channel algorithms, the data are low quality, and there is no overlap to intercalibrate the data with the 1978–present record. Cavalieri et al. (2003) produced a total extent timeseries from the combined ESMR-SMMR-SSM/I record by using operational ice charts from the US National Ice Center (Dedrick et al., 2001) as a "bridge" between ESMR and the SMMR-SSM/I period. The National Ice Center ice chart climatology records weekly sea ice information since 1972 based on human analysis of available satellite imagery and reconnaissance. The Canadian Ice Service also has compiled a climatology of their charts since 1968 for Canadian waters (Tivy et al., 2011). However, particularly during the 1970s, satellite imagery was limited and the ice charts were often based on climatology and the analysts' knowledge of the sea ice environment. Finally, a climatology has been produced from Russian ice charts for Russian waters from the early 1930s (Mahoney et al., 2008).

TCD
7, 35–53, 2013

Another long-term sea ice product has been produced by the UK Hadley Centre (Rayner et al., 2003). This product compiled a record of sea ice since 1870 for input to climate models, based on a climatology compiled by Walsh and Chapman (2001), passive microwave data, and other sources. However, much of the record in the Arctic before 1953 and the Antarctic before 1972 was simply an average climatology. In addition, there is not any overlap between the Walsh and Chapman climatology and the passive microwave record, so a discontinuity exists leading to uncertainty in trends. However, the dataset has been used to examine trends since 1953 (Meier et al., 2007, 2012) and compare with model estimates (Stroeve et al., 2007).

These records provide useful, albeit incomplete, information to supplement the high quality multi-channel passive microwave record. Nonetheless, there is the desire to add to and improve these estimates. There was a substantial amount of satellite data collected from the early 1960s through the mid-1970s that are potentially useable, but which have not been available and/or not been sufficiently analyzed to be of use. Here we present initial data from the Nimbus I satellite that can provide new estimates of Arctic and Antarctic sea ice extent during September 1964.

2 Nimbus I satellite data

The era of visible earth remote sensing began with the launch of the NASA Nimbus I in August 1964. It carried the Advanced Vidicon Camera System (AVCS) and other sensors. Nimbus I was followed by Nimbus II (operated from 15 May 1966–18 January 1969) and Nimbus III (14 April 1969–22 January 1972). Thus, the current sea ice satellite record for 1979–present can be extended, at least sporadically, 15 yr further back in time.

These early sensor data were not used extensively, not because of data quality issues, but rather due limitations of computation power and processing speed and because the idea of collecting climate data was not a focus until later.

TCD
7, 35–53, 2013

Here we analyze data from the Nimbus I AVCS sensor and demonstrate the ability to obtain useful sea ice extent estimates as well as other potential information on the sea ice cover. The AVCS used video technology to collect snapshots every 91 s. These were transmitted to earth receiving stations as analog TV images, which were then photographed onto 35 mm film. The presence of clouds limits the ability to observe the sea ice surface with the AVCS, but over the three weeks we were able to produce composites of largely clear-sky images covering most of the Arctic and Antarctic basins.

The Nimbus I operated for only 3 weeks after launch, providing data from 30 August to 19 September 1964. However, this fortunately coincides with the September minimum sea ice extent in the Arctic and the maximum extent in the Antarctic. This is a time period of particular interest for both hemispheres. In the Arctic, the Nimbus data provide a longer-term context for the dramatic decline in sea ice extent since 1979 observed in multi-channel passive microwave data.

In the Antarctic, September is a period where the intriguing Weddell Sea polynya feature was seen in early passive microwave satellite data during 1974–1976. Polynyas are semi-persistent areas of open water within the ice pack driven either by persistent winds pushing ice away from a barrier such as land, fast ice, or an ice shelf (latent heat), or by upwelling ocean heat (sensible heat) (Morales Maqueda et al., 2004). Latent heat polynyas are common features along the Antarctic coast due to persistent off-shore winds coming down off the ice sheet. However, the Weddell Sea polynya was a sensible heat polynya well away from the coast. After being a prominent late winter feature during 1974–1976, it has not been observed to the same degree since. The early Nimbus satellite data has the potential to determine if the polynya existed before 1974.

TCD
7, 35–53, 2013

3 Methodology

3.1 Recovery and processing of imagery

The process of creating Arctic and Antarctic extent maps began with recovery of the data by the NASA Goddard Space Flight Center (GSFC). The Nimbus I AVCS data was archived on 35 mm film rolls. Each frame in the film was scanned at an 8-bit sampling range (higher than the 4-bit resolution of the original film) using a Kodak HR500 high-speed film scanner. A procedure was implemented to create automated metadata to document the imagery as they were scanned. Over 13 000 images were digitized from Nimbus I.

Although most images have a gray-scale to aid in calibration, the camera sensitivity varied during the orbit, making absolute calibration impossible. In addition, the spectral range of the imagery as recorded by the camera corresponds to 4-bit resolution at best. Thus contrast and between high and low reflectance is limited and many fine details (e.g. cloud features) are not evident. However, the imagery is suitable to delineate between the darker ocean and the lighter ice. And, in general, clouds can be distinguished from the ice cover.

3.2 Retrieval of ice extent

Sea ice extent was retrieved by analyzing suitable images near the ice edge. An initial approach composited individual images based on a minimum brightness criteria to filter out cloud-covered images and retrieve a "clear-sky" composite. This provided an initial qualitative indication of the ice-covered region (Fig. 1). However, variations in calibration and other ambiguities in the imagery precluded an automated quantitative estimate of the ice edge using this method. Thus, manual analysis was used to select the ice edge in individual images.

Images with useful clear-sky regions where an ice edge was visible were analyzed and then composited into the Arctic and Antarctic fields. Overall, roughly 1000 images

TCD
7, 35–53, 2013

were reviewed to identify the ice edge boundaries. The composited basin-wide fields were created from images throughout the three week period of data acquisition. Thus, the resulting composite is not a snapshot of ice extent, nor does it reflect a true average over the three week period. Nonetheless, the composite ice edges provide a good representation of the ice cover during the sampling period.

4 Results and evaluation

4.1 Antarctic extent

Near-complete coverage of the Antarctic ice edge was possible over the course of the three weeks of imagery. There are uncertainties in the edge position because of ambiguities in the imagery and limitations of the manual analysis. However, in many regions, an ice edge was quite clear and the position could be established with high confidence (Fig. 2). Another important factor in deriving the ice edge is that imagery was collected over a three week period. Thus some differences in ice edge location are due to the change in the position of the ice edge during the period of image collection. We accounted for regions with uncertainty by marking multiple ice edges – a northern edge and a southern edge. This results in a "bracketing" of the ice extent value and provides a range of uncertainty in the September average.

Our analysis for September 1964 yields a realistic ice edge (Fig. 3) in comparison with passive microwave data, based on the September 1979–2000 average ice edge from the NSIDC Sea Ice Index (Fetterer et al., 2009). The bounds between the more northerly and more southerly edge represent multiple views of this area on different days. In some places, such as north of the Weddell Sea, there is little discrepancy and the edge location, indicating a stable and clearly defined ice edge. In other areas, such as in the Indian Ocean sector, there are large discrepancies, indicating ambiguities in the imagery and/or large temporal variation in the ice edge location.

TCD
7, 35–53, 2013

Sea ice extent is calculated by summing the area within the contours, not including land, ice sheet, or ice shelf. The total Antarctic extent for September 1964 is estimated to be 19.7×10^6 km^2, with an uncertainty range of 18.3 and 21.2×10^6 km^2 between the northerly and southerly estimates. There are no corroborating ship and aircraft data available to validate our estimate. However, our average estimate is in good agreement with a 1960s era estimate of 19.81×10^6 km^2 by Predoehl (1966).

Notably, our 1964 estimate is substantially higher than the estimates within the passive microwave record (Fig. 4). Even within the wide range of uncertainty in the Nimbus I estimate, the extent is higher than the monthly September average of any of the years of the passive microwave record (1979–2012). Even taking into consideration variation over the month and using the highest and lowest daily extent values during September, the Nimbus I value is clearly on the highest end of the estimates. This suggests that the Antarctic sea ice was more extensive during the 1960s and the small increasing trend during the 1979–2012 period may reflect long-term variability as the ice cover recovers from a relatively low level back to 1960s conditions.

As mentioned above, an intriguing feature in early passive microwave imagery is the Weddell Sea polynya that was observed in 1974–1976 and has not been seen to the same degree since. Our analysis of Nimbus I imagery does not show a clear polynya in the region in 1964. However, there were only 8 views of any given region over the three weeks and it is difficult to distinguish homogeneous clouds from homogeneous ice within the pack. There is some indication of reduced ice concentration that could be indicative of a polynya feature in some imagery (Fig. 5), but it is not conclusive. Future analysis of Nimbus II and III imagery may yield indications of the possible existence of the polynya in those years.

4.2 Arctic extent

Determining a September 1964 sea ice extent for the Arctic was more difficult than for the Antarctic. One reason is because of limited coverage and difficulty in distinguishing the ice edge along the coasts from snow or glacier-covered islands in the

TCD
7, 35–53, 2013

Canadian Archipelago. Another limitation was the lack of data north of Alaska and eastern Siberia because data was downloaded to the Alaska Receiving Station at Fairbanks and simultaneous collection and relaying of data was not possible. The available imagery covered a region extending from the Kara Sea westward across the Barents Sea, Fram Strait, the Canadian Archipelago to the eastern part of the Beaufort Sea. Fortunately, unlike in the Antarctic, there are other sources of extent data that can fill in the gaps in the Nimbus I coverage and provide independent comparison in regions of overlap. We compared our Nimbus I estimates with Russian (AARI, 2007) and Alaskan (NSIDC/WDC, 2005) ice charts. Where Nimbus I estimates overlap with estimates from the ice charts, there is generally good agreement between the edge of the drifting ice. The Russian ice charts also marked narrow areas of fast ice along the Siberian coast, which we did not include in our estimates.

Combining all three sources, we map the ice edge throughout most of the Arctic basin, excluding the region between 233 and 340° E longitude, primarily encompassing the Canadian Archipelago (because of the lack of useable Nimbus I imagery in that region or ambiguity in the imagery, such as flaw leads near the coast) (Fig. 6). We filled this region with the average of the 1979–2000 extent from the passive microwave record, $1.76 \times 10^6\,\mathrm{km}^2$, obtain a total Arctic sea ice extent. Summing the total extent within the Arctic basin yields an estimate of $6.90 \pm 0.3 \times 10^6\,\mathrm{km}^2$. This compares to a total extent from the median 1979–2000 extent from the Sea Ice Index of $7.04 \times 10^6\,\mathrm{km}^2$. Overall then, the 1964 estimate is reasonably consistent with the 1979–2000 conditions, with the 1964 estimate falling with the range of extents during the passive microwave era (Fig. 7). This suggests that September extent in the Arctic may have been generally stable through the 1960s and early 1970s, though more years of data are needed to confirm this.

TCD
7, 35–53, 2013

5 Conclusions

New maps of the sea ice edge and estimates of total ice extent in the Arctic and Antarctic during September 1964 have been produced from Nimbus I satellite data. Overall the estimates agree with other data sets and analyses, giving us confidence that our approach yields reasonable estimates that can be extended to other early satellite data. Within our measurement precision we demonstrate that 1964 Antarctic ice extent is likely higher than any year observed from 1972 to 2012 to present. We plan to analyze imagery from the subsequent Nimbus II and III satellites as well as other available data from satellites operating in the late 1960s and early 1970s. These have the potential to provide monthly estimates of sea ice extent through much of the period between 1964 and the start of the multi-channel passive microwave era in 1979. This will yield a climate record of sea ice approaching 50 yr in length that will put the recent changes, especially the dramatic decline of Arctic summer sea ice extent, in a longer-term context. These data will also be extremely valuable for validation of climate modeling simulations.

The digitized data used in this study and future research is being documented, compiled into a useable format, and will be archived at distributed by NSIDC.

Acknowledgements. This research was fund by a sub-contract to NASA grant #NNG08HZ07C. We also thank the students Carl Gallaher and Alex Calder for the diligence in scanning and documenting the 13 000 images used in this study.

References

AARI: Sea ice charts of the Russian Arctic in gridded format, 1933–2006, Arctic and Antarctic Research Institute, edited and compiled by: Smolyanitsky, V., Borodachev, V., Mahoney, A., Fetterer, F., and Barry, R., National Snow and Ice Data Center, Boulder, Colorado, USA, Digital media, 2007.

Cavalieri, D. J. and Parkinson, C. L.: Antarctic sea ice variability and trends, 1979–2006, J. Geophys. Res., 113, C07004, doi:10.1029/2007JC004564, 2008.

TCD
7, 35–53, 2013

Cavalieri, D. J., Gloersen, P. and Campbell, W. J.: Determination of sea ice parameters with the NIMBUS-7 SMMR, J. Geophys. Res., 89, 5355–5369, 1984.
Cavalieri, D. J., Parkinson, C., Gloersen, P., Comiso, J., and Zwally, H. J.: Deriving long-term time series of sea ice cover from satellite passive-microwave multisensor data sets, J. Geophys. Res., 104, 15803–15814, 1999.
Cavalieri, D. J., Parkinson, C. L., and Vinnikov, K. Y.: 30-Year satellite record reveals contrasting Arctic and Antarctic decadal sea ice variability, Geophys. Res. Lett., 30, 1970, doi:10.1029/2003GL018031, 2003.
Cavalieri, D. J., Parkinson, C., DiGirolamo, N., and Ivanov, A.: Intersensor calibration between F13 SSM/I and F17 SSMIS for global sea ice data records, IEEE T Geosci. Remote Sens. Lett., 9, 233–236, 2012.
Comiso, J. C.: Characteristics of arctic winter sea ice from satellite multispectral microwave observations, J. Geophys. Res., 91, 975–994, 1986.
Comiso, J. C. and Nishio, F.: Trends in the sea ice cover using enhanced and compatible AMSR-E, SSM/I, and SMMR data, J. Geophys. Res., 113, C02S07, doi:10.1029/2007JC004325, 2008.
Dedrick, K. R., Partington, K., Van Woert, M., Bertoia, C. A., and Benner, D.: US National/Navy Ice Center digital sea ice data and climatology, Can. J. Remote Sens., 27, 457–475, 2001.
Fetterer, F., Knowles, K., Meier, W., and Savoie, M.: Sea Ice Index, National Snow and Ice Data Center, Boulder, Colorado, USA, Digital media, 2002, updated 2009.
Mahoney, A. R., Barry, R. G., Smolyanitsky, V., and Fetterer, F.: Observed sea ice extent in the Russian Arctic, 1933–2006, J. Geophys. Res., 113, C11005, doi:10.1029/2008JC004830, 2008.
Meier, W. N., Stroeve, J., and Fetterer, F.: Whither Arctic sea ice? A clear signal of decline regionally, seasonally and extending beyond the satellite record, Ann. Glaciol., 46, 428–434, 2007.
Meier, W. N., Stroeve, J., Barrett, A., and Fetterer, F.: A simple approach to providing a more consistent Arctic sea ice extent time series from the 1950s to present, The Cryosphere, 6, 1359–1368, doi:10.5194/tc-6-1359-2012, 2012.
Morales Maqueda, M. A., Willmott, A. J., and Biggs, N. R. T.: Polynya dynamics: a review of observations and modeling, Rev. Geophys., 42, RG1004, doi:10.1029/2002RG000116, 2004.

TCD
7, 35–53, 2013

NSIDC/WDC for Glaciology, Boulder, compiler: The Dehn collection of Arctic sea ice charts, 1953–1986, National Snow and Ice Data Center/World Data Center for Glaciology, Boulder, Colorado, USA, Digital media, 2005.

Parkinson, C. L. and Cavalieri, D. J.: Arctic sea ice variability and trends, 1979–2006, J. Geophys. Res., 113, C07003, doi:10.1029/2007JC004558, 2008.

Predoehl, M.: Antarctic pack ice: boundaries established from Nimbus I pictures, Science, 153, 861–863, 1966.

Rayner, N. A., Parker, D. E., Horton, E. B., Folland, C. K., Alexander, L. V., Rowell, D. P., Kent, E. C., and Kaplan, A.: Global analyses of sea surface temperature, sea ice, and night marine air temperature since the late nineteenth century, J. Geophys. Res., 108, 4407, doi:10.1029/2002JD002670, 2003.

Stroeve, J., Holland. M. M., Meier, W., Scambos, T., and Serreze, M.: Arctic sea ice decline: faster than forecast, Geophys. Res. Lett., 34, L09501, doi:10.1029/2007GL029703, 2007.

Tivy, A., Howell, S. E. L., Alt, B., McCourt, S., Chagnon, R., Crocker, G., Carrieres, T., and Yackel, J. J.: Trends and variability in summer sea ice cover in the Canadian Arctic based on the Canadian Ice Service Digital Archive, 1960–2008 and 1968–2008, J. Geophys. Res., 116, C03007, doi:10.1029/2009JC005855, 2011.

Walsh, J. E. and Chapman, W. L.: Twentieth-century sea ice variations from observational data, Ann. Glaciol., 33, 444–448, 2001.

TCD

7, 35–53, 2013

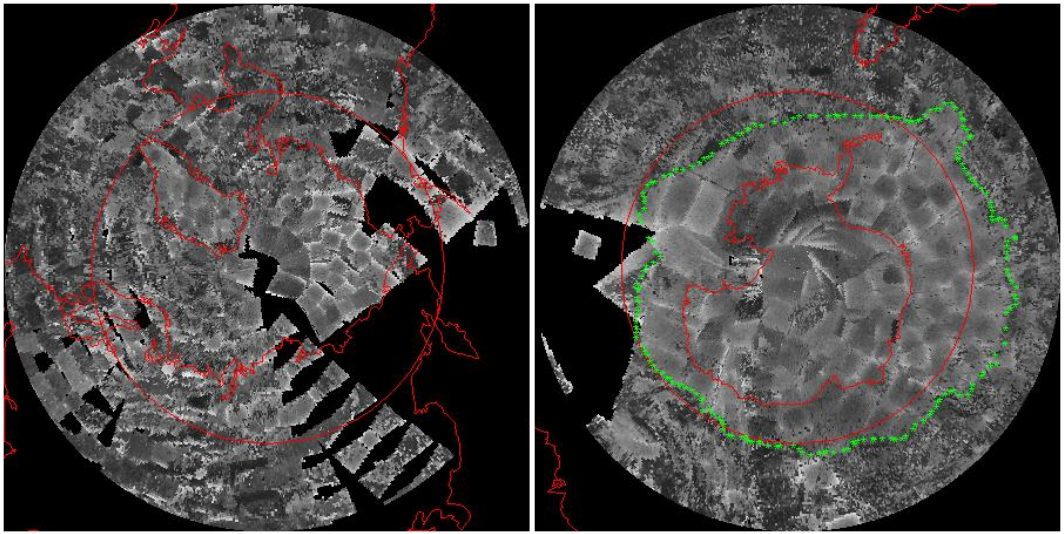

Fig. 1. Composite of Arctic (left) and Antarctic (right) region from Nimbus I AVCS imagery using a minimum brightness criteria. In some regions, the brighter sea ice is clearly distinguished from the darker ocean, but there are ambiguities at many locations that make automated delineation of an ice edge difficult.

TCD
7, 35–53, 2013

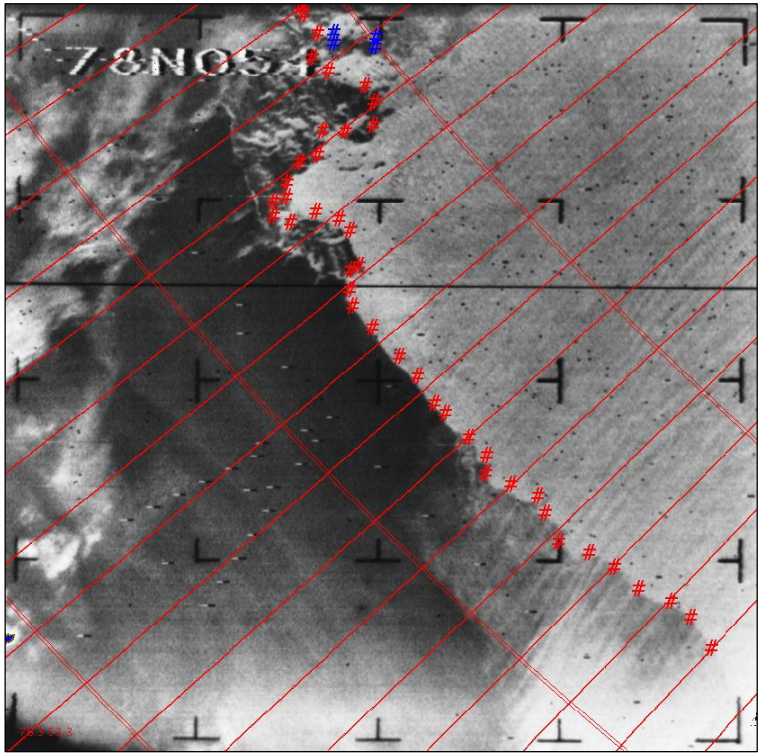

Fig. 2. Sample image of the Arctic ice edge north of Russia near Franz Josef Land (centered at 78° N and 54° E) on 4 September 1964. The estimated boundary between the ice and ocean is marked by red "#" marks; openings (leads) within the ice are marked by blue "#".

TCD
7, 35–53, 2013

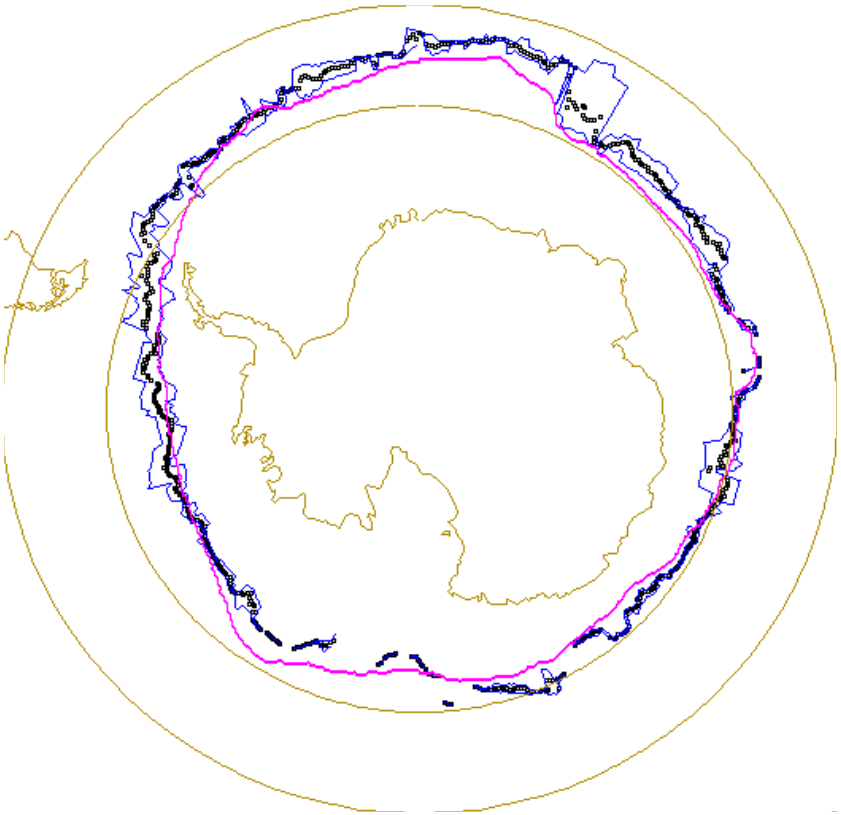

Fig. 3. Outline of Antarctic sea ice edge from Nimbus I AVCS imagery using manual analysis. Solid blue lines represent minimum (more southern) and maximum (more northern) estimates of the ice edge in the manual analysis. Black dots represent the average or "best-estimate" of the ice edge. The pink line is the 1979–2000 median ice edge from the passive microwave-based NSIDC Sea Ice Index product.

TCD
7, 35–53, 2013

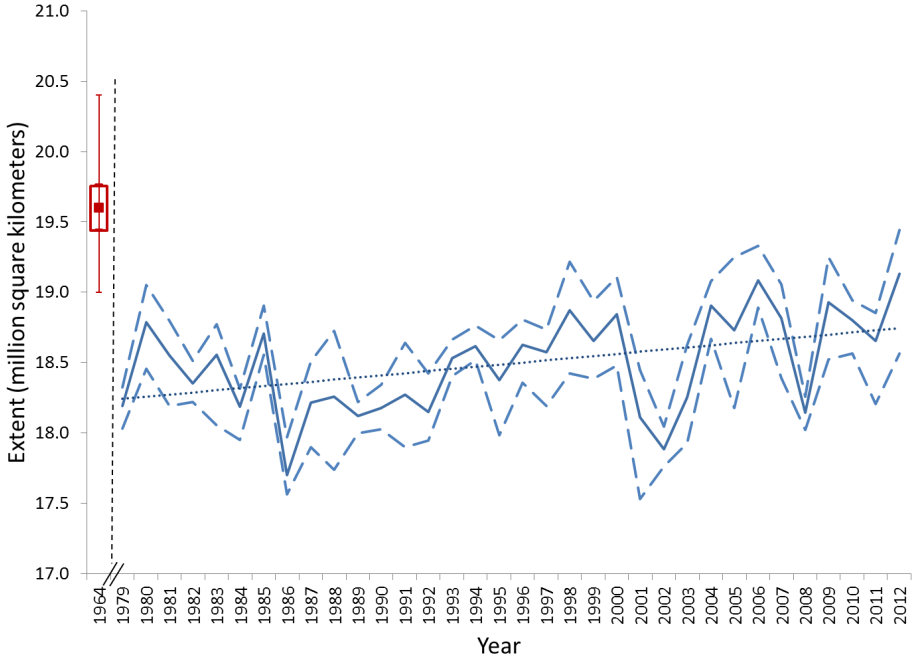

Fig. 4. Timeseries of Antarctic September sea ice extent. The Nimbus I estimate for 1964 is to the left in red as a box and whisker plot with the passive microwave NSIDC Sea Ice Index values for 1979–2011. For Nimbus, the box represents the standard deviation of the different edge locations, which the whiskers represent the absolute maximum and minimum range. The blue solid line is the monthly average passive microwave September values, while the blue dashed lines represent a three-day average of the high and low range of daily extents during the month.

TCD
7, 35–53, 2013

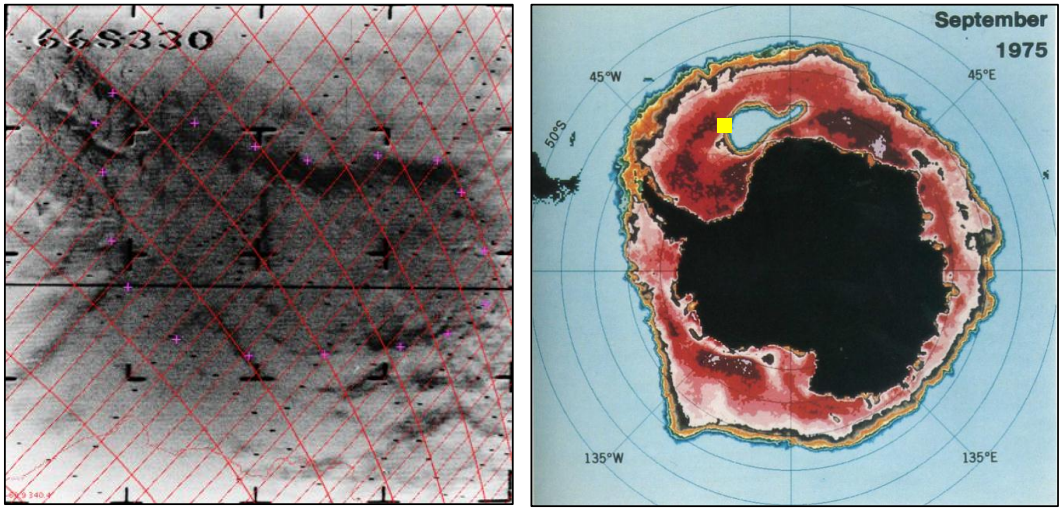

Fig. 5. Nimbus II imagery from the region of the Weddell Sea polynya (66° S, 330° E) in September 1964 (left), and the polynya seen in passive microwave imagery in September 1975 (right); the yellow square indicates the location of the 1964 scene. The dark features in the Nimbus II image indicate potential low ice concentration and the darkest areas appear to be open water. However, it is not clear if there was a polynya at or near the time of the image or just an indication of leads and clouds.

TCD
7, 35–53, 2013

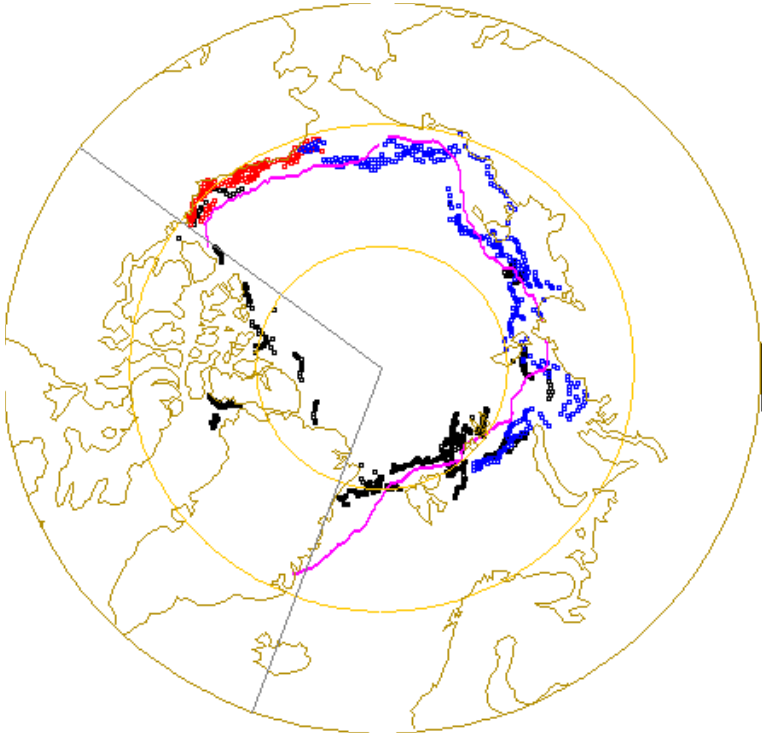

Fig. 6. Outline of September 1964 Arctic sea ice edge from Nimbus I (black dots), Alaskan ice charts (red), and Russian ice charts (blue). The pink line is the 1979–2000 median ice edge from the passive microwave-based NSIDC Sea Ice Index product. The straight gray lines indicate the region filled in by the 1979–2000 average extent from the Sea Ice Index.

TCD
7, 35–53, 2013

Fig. 7. Timeseries of Arctic September sea ice extent. The combined estimate for 1964 from the Nimbus imagery and the Russian and Alaskan ice charts is to the left with the passive microwave NSIDC Sea Ice Index values for 1979–2011. For Nimbus, the error bars represent the standard deviation of the estimates. The blue solid line is the monthly average passive microwave September values, while the blue dashed lines represent a three-day average of the high and low range of daily extents during the month.

TCD
7, 35–53, 2013